NASA TECHNICAL MEMORANDUM

NASA TM X-2420

NASA TM X-2420

PERFORMANCE OF AN ELECTRICALLY RAISED, SYNCHRONOUS SATELLITE WHEN SUBJECTED TO RADIATION DEGRADATION EFFECTS

by James E. Cake and John D. Regetz, Jr.

Lewis Research Center
Cleveland, Ohio 44135

NATIONAL AERONAUTICS AND SPACE ADMINISTRATION • WASHINGTON, D. C. • NOVEMBER 1971

1. Report No.	2. Government Accession No.	3. Recipient's Catalog No.
NASA TM X-2420		

4. Title and Subtitle	5. Report Date
PERFORMANCE OF AN ELECTRICALLY RAISED, SYNCHRONOUS SATELLITE WHEN SUBJECTED TO RADIATION DEGRADATION EFFECTS	November 1971
	6. Performing Organization Code

7. Author(s)	8. Performing Organization Report No.
James E. Cake and John D. Regetz, Jr.	E-6477
	10. Work Unit No. 682-10

9. Performing Organization Name and Address	11. Contract or Grant No.
Lewis Research Center National Aeronautics and Space Administration Cleveland, Ohio 44135	
	13. Type of Report and Period Covered
12. Sponsoring Agency Name and Address	Technical Memorandum
National Aeronautics and Space Administration Washington, D.C. 20546	14. Sponsoring Agency Code

15. Supplementary Notes

16. Abstract

The use of solar electric propulsion to raise a high-power communication satellite from a low altitude, inclined circular orbit to the geosynchronous orbit is evaluated. Since the satellite ascends through the high intensity radiation belts, the power available from the solar array and therefore to the ion thrusters degrades. The performance of the solar electric stage in combination with the thrust augmented Thor/Delta launch vehicle is evaluated for two thrust steering programs. The transfer times and solar array requirements are presented for total geosynchronous payloads from 450 to 1100 kg.

17. Key Words (Suggested by Author(s))	18. Distribution Statement
Low-thrust propulsion, Electric propulsion, Communications satellite, Synchronous satellite, Solar cell degradation	Unclassified - unlimited

19. Security Classif. (of this report)	20. Security Classif. (of this page)	21. No. of Pages	22. Price*
Unclassified	Unclassified	21	$3.00

* For sale by the National Technical Information Service, Springfield, Virginia 22151

PERFORMANCE OF AN ELECTRICALLY RAISED, SYNCHRONOUS SATELLITE WHEN SUBJECTED TO RADIATION DEGRADATION EFFECTS

by James E. Cake and John D. Regetz, Jr.

Lewis Research Center

SUMMARY

The use of solar electric propulsion to raise a high-power communication satellite from a subsynchronous to the geosynchronous orbit is evaluated. The photovoltaic power source must provide at least 5 kilowatts of power during the ascent trajectory and during 5 years of operation in geosynchronous orbit. As the satellite ascends through the high intensity radiation belts, the power available from the solar array and therefore available to the ion thrusters degrades. Background for the space radiation effect and the technique for calculating the degradation to the solar array are given.

The spacecraft is assumed to be injected into a low altitude, inclined circular orbit by a thrust augmented Thor/Delta launch vehicle. The performance of the electric stage in combination with this launch vehicle is evaluated for achievement of geosynchronous orbit with two thrust vector controls or steering programs. The first program changes the orbital altitude and inclination sequentially, while the second program changes these elements concurrently and is a near optimal solution.

For both steering programs, the transfer times and solar array size requirements are presented for total geosynchronous payloads from 450 to 1100 kilograms. Compared on the basis of total geosynchronous payload, the second steering program offers a 22 to 25 percent decrease in the transfer time over that of the first steering program. The second steering program, however, requires a slightly larger (up to 2 percent) solar array. For a geosynchronous payload range from 450 to 1100 kilograms, the transfer times for the second steering program vary from 90 to 285 days. Over the same payload range, 8.5 to 10 kilowatts of solar array are required to produce a degraded solar array power of 5 kilowatts after 5 years of operation. This compares to an initial solar array of 7 kilowatts required for a direct injection mission.

INTRODUCTION

The use of electric propulsion to raise a high-power communications satellite from a low Earth orbit to a geosynchronous orbit has been discussed for some time. A photovoltaic power source provides both the power for the electric stage during the ascent trajectory and the power for the communication experiments at geosynchronous orbit. Achievement of the geosynchronous orbit with sufficient power to operate the experiments for the desired lifetime is strongly dependent on the space radiation received by the power source both during the ascent and the on-orbit operations.

Some previous solar electric propulsion studies have assumed that the power available to the ion thrusters is constant during the ascent. In references 1 to 3, either the solar array degradation was assumed to be negligible or the additional array required to compensate for the degradation was not employed by the thrusters. This report presents some results of a spiral-out to geosynchronous orbit when the power to the thrusters is varied to correspond to the existing array power.

The launch vehicle chosen for this study is the thrust augmented Thor/Delta. The first stage is a long tank Thor with nine Castor II solid rocket motors for thrust augmentation. In the second stage Delta, the Titan transtage engine replaces the Delta engine. The electric stage is substituted for the normal third stage solid motor.

The electric stage is injected into a low altitude, circular parking orbit with a 28.5° inclination. Two types of thrust vector control for the electric stage are considered for placing the spacecraft into the geosynchronous orbit. The first is the sequential program where the altitude is increased to the synchronous altitude, followed by the reduction of the inclination. The second type of thrust vector control concurrently changes the altitude and inclination, as suggested by Edelbaum in reference 4, such that the end conditions of altitude and inclination are reached simultaneously. Time penalties incurred by Earth shadowing of the spacecraft are presented for both thrust control types.

An ion thruster using a single set of operating characteristics was selected for the entire payload range rather than optimizing the operating characteristics for each payload and trajectory. These characteristics represent an ion thruster consistent with the technology available for a middle to late 1970 launch date.

The main outcome of the study will be the transfer times required to place a range of payloads into the geosynchronous orbit for the two thrust control types. Also defined will be the initial solar array size requirements based on the degradation assumed.

ANALYSIS

Mission Definition

The problem given is to define the trajectory and calculate the performance for a high-power communications satellite to be injected into geosynchronous orbit by means of electric propulsion. The spacecraft is first assumed to be injected into a low altitude, inclined circular orbit by a TAT(9C)/Delta launch vehicle. The principal reason for the choice of this launch vehicle is its relative economy. A solar array is used to power the ion thrusters during the ascent and then the communications experiments once in geosynchronous orbit. Since the solar array output power degrades while traversing the radiation belts, a method is required for calculating the degraded solar array power and the resulting available thrust from the ion thrusters. The ascent trajectory to geosynchronous orbit and the resulting electric stage performance can then be defined for a given method of thrust vector control.

Radiation Degradation Background

A spacecraft in a spiral-out trajectory to the geosynchronous orbit is subjected to the damaging effects of the trapped electron and proton environments of the radiation belts. Upon reaching the geosynchronous orbit, trapped electrons and solar flare protons continue to impinge on the solar array. Figure 1 shows an example of a trapped proton and electron flux map. In the geosynchronous orbit, the damage rate to the solar cell is dependent on the flux which in turn is a function of solar activity. The damage rate during the ascent trajectory is not only a function of the solar activity, but also of the spacecraft's position in the trapped radiation belt as can be seen from figure 1. The solar array damage incurred at every orbit revolution during the ascent is a function of the time spent at a particular damage rate.

As mentioned previously, the performance of this launch vehicle-electric stage combination will be evaluated for the case where the ion thrust is varied according to the power available from the solar array. We therefore desire to calculate the damage to the solar array at small time increments during the ascent, for instance at every orbit revolution. Adjusting or throttling the thrusters for the next revolution will allow us to calculate the trajectory which results from using the maximum thrust available on each orbit revolution.

The mathematical model of the degradation calculation is defined subsequently. The reader is directed to a more thorough treatment of radiation damage to solar cells found in references 5 and 6.

The effect of penetrating radiation on a silicon solar cell is to increase the number of crystal defects, otherwise known as recombination centers for minority carriers. The performance parameters of solar cells are assumed to be unique functions of the minority carrier diffusion length. From reference 5, the minority carrier diffusion length is defined as the average distance traversed by the photon generated carriers before being reduced to a factor of 1/e (where e is the base of the natural logarithm) of their original number through recombination processes. As the radiation continues to penetrate, more recombination centers continue to form such that fewer minority carriers reach the p-n junction of the cell but rather recombine with a majority carrier at the crystal defect. Since fewer minority carriers reach the junction, less electrical power results.

The additional assumption that the space radiation causes a uniform reduction in the minority carrier diffusion length throughout the base region allows the new power to be calculated by a simple expression. The decrease in the minority carrier diffusion length of a solar cell is described by

$$\frac{1}{L^2} = \frac{1}{L_o^2} + d_\tau t \tag{1}$$

where L is the minority carrier diffusion length in centimeters, d_τ the damage rate, and t the number of days the solar cell has been at the damage rate d_τ. For this study, the value of the diffusion length for an unexposed array is assumed to be 200 microns, which is consistent with reference 5. Figure 2 shows the damage rate of equation (1) which consists of electron, proton, and solar flare damage rates. The damage rates, which are for a 30^o inclined orbit, assume that the flux of electrons and protons is isotropic. Vette's model of the trapped radiation environment was used in the construction of the damage rate curve. The curve is valid for n/p solar cells having a base resistivity of 10 ohm-centimeters with 6 mil fused silica coverglass frontal protection and an equivalent backside protection.

From reference 5, the maximum power ratio of a solar cell of a certain base resistivity correlates with the minority carrier diffusion length. For the 10 ohm-centimeter base resistivity solar cells used in this study, the maximum power ratio has been determined in the laboratory to be described by

$$\frac{Pm}{Pmo} = 0.20 + 0.35 \log_{10} L \tag{2}$$

where L is in microns. The digital simulation for the low thrust trajectory, as discussed in the appendix, calculates the changes in the orbital elements after each orbit revolution. Then, the current values of the minority carrier diffusion length (eq. (1))

and the maximum power ratios (eq. (2)) are computed to determine the available thrust for the next orbit revolution. Only one table of damage rate, figure 2, which is for an inclination angle of 30^{o}, is used for this calculation. This may result in some error in the degradation calculation when considering the thrust vector control method which concurrently changes the altitude and inclination. The error is negligible for the sequential thrust vector control method since the inclination changing occurs only at the geosynchronous altitude where there is little latitude dependence of damage rate.

The performance of the launch vehicle/electric stage as given later in the report is subject to uncertainties in the particle environments and the validity of the method for calculating d_{τ}, L, and Pm/Pmo. Physical characteristics of the solar cell such as coverglass thickness, cell thickness, and the base resistivity will also influence the performance.

This study considers only the effect of radiation degradation on the performance of the solar cell. Although this is the dominant effect, those of coverslide darkening, temperature changes, thermal cycling, and micrometeoroid erosion may be worthy of consideration in a more detailed analysis.

Assumptions

The assumptions made in this study are now presented in detail.

Solar array. - The solar array is required to provide 5 kilowatts of power at the completion of 5 years geosynchronous operation. During the ascent, the solar array is maintained normal to the Sunline to provide maximum power available.

Launch vehicle. - The launch vehicle used to establish the initial parking orbit is the thrust augmented Thor/Delta. The first stage is a long tank Thor with nine Castor II solid rocket motors for thrust augmentation. In the second stage Delta, the Titan transtage engine replaces the Delta engine. A third stage solid motor is not used, thereby providing more payload envelope within the 57 inch (1.45 m) standard Delta shroud although some of this space will be required for the electric thruster system. The performance of the launch vehicle is presented in figure 3. The results assume parking orbit achievement by means of a Hohmann transfer orbit from a 100 nautical mile (185 km) circular orbit, no second stage propellant reserves, and a 34 kilogram attach fitting which is excluded from the curve of figure 3.

Orbit shape. - Since the thrust to weight ratio is sufficiently small, the orbits remain circular throughout the ascent trajectory.

Orbit shadowing considerations. - For missions starting with a parking orbit altitude of below approximately 7000 kilometers, the possibility exists for Earth shadowing of the spacecraft once per orbit at some time or times during the ascent trajectory.

Therefore, a check is made at the start of every orbit revolution to determine whether shadowing will be incurred. The geometry of the shadow is assumed to be a cylinder and the orbits remain circular. Therefore, when the following condition is satisfied, the spacecraft is in shadow:

$$\cos \eta < \frac{R}{R + H} \tag{3}$$

where η is the angle between the angular momentum vector and the sunline, R the equatorial radius, and H the orbit altitude. If equation (3) is satisfied, the shadow entrance and exit values are calculated and thrusting is terminated for that portion of the orbit in the digital calculation.

Ion thruster characteristics. - The ion thrusters selected for this study represent a compromise design for a particular synchronous payload range. Each of the three thrusters used in the analysis has an initial and maximum input power of 2.5 kilowatts. The initial specific impulse of 2500 seconds was chosen since it met an 800 volt minimum beam voltage requirement and was in the neighborhood of the optimum specific impulse as shown in reference 7. The thrusters are representative of a class of thrusters having an anode diameter of 30 centimeters with the single accelerator grid being ceramic coated to maintain a high electrical efficiency. The initial ion thruster parameters are listed in table I. For the stated input power and thruster specific impulse, the initial beam current required represents technology expected to be available in the middle to late 1970's. It is assumed that the ion thruster development program will yield an increase in the present, maximum beam current. Slight modification of the anode diameter could compensate for any advancement not achieved through the development program. Likewise, the losses and efficiencies are subject to progress made in the development program.

The throttling technique, presented in table II, maintains a constant beam voltage while varying the beam current. A detailed background for the throttling procedure may be found in references 8 and 9. The large degradation in propellant utilization efficiency with decreases in the beam current is also expected to be improved with the research and development program. The current and voltage of table II are not calculated from a degraded current-voltage characteristic curve. Rather, the current and voltage are obtained from the maximum power available as calculated by equations (1) and (2).

Orbit Transfer with a Sequential Thrust Control

One method of achieving geosynchronous orbit from a low altitude, inclined parking orbit is to independently change the orbital elements by a specified procedure. The first

step is to increase the semimajor axis to the geosynchronous value. This maneuver is followed by removing any residual eccentricity and then by reducing the inclination to zero. The thrust vector control method employed to achieve these maneuvers is presented in figure 4. Figure 4(a) shows the circumferential thrust program for the semimajor axis change, and figure 4(b) shows the normal thrust reversing directions at the antinodes for inclination changing alone. The appendix contains the equations for the changes in the orbital elements which are used in the digital computer program for the trajectory calculation. The control angle, the out-of-plane angle between the velocity vector and the thrust vector, is set to 0° for the circumferential thrust and to 90° for pure normal thrust. Eccentricity removal requires an independent equation.

Some of the reasons for choosing a thrust vector control sequence that first raises the orbit and then changes the inclination should be obvious. First, the characteristic velocity requirements for changing the inclination and eccentricity are greater at altitudes below the geosynchronous. In addition, because more time would be spent at the lower altitudes, the solar array would suffer more degradation, and longer periods of Earth shadowing would be incurred.

Orbit Transfer with a Near Optimal Thrust Control

The second method of achieving geosynchronous orbit considered is to maintain a thrust vector control which concurrently changes the orbital semimajor axis and inclination. The thrust vector control, shown in figure 5, causes the end conditions of semimajor axis and inclination to be reached simultaneously. The control angle β is a constant over one orbit period with the out-of-plane direction of the thrust vector being changed at the antinodes. This represents a near optimal solution compared to the true optimal solution where the control angle is varied through each orbit revolution. The true optimal solution cannot, however, be carried out in a closed form as the near optimal solution was for this study.

The initial and updated values of the control angle are calculated according to the following procedure which was derived in reference 4. First, the characteristic velocity required to simultaneously remove the inclination Δi and increase the semimajor axis to geosynchronous is calculated by

$$\Delta V = \left(V_o^2 - 2V_f V_o \cos \frac{\pi}{2} \Delta i + V_f^2\right)^{1/2} \tag{4}$$

The initial control angle β_o using this result is found by solving the transcendental equation

$$\Delta i = \frac{2}{\pi} \sin^{-1} \left(\frac{V_o \sin \beta_o}{V_o^2 - 2V_o \Delta V \cos \beta_o + \Delta V^2} \right) - \frac{2\beta_o}{\pi} \tag{5}$$

The control angle is updated on successive orbits according to

$$TV \sin \beta = T_o V_o \sin \beta_o \tag{6}$$

where the thrust T is an additional parameter to the control law established by Edelbaum ($V \sin \beta = V_o \sin \beta_o$). The basis for this addition is that since the thrust is continually decreasing, the control angle β needs to be larger to effect the same change in inclination had the thrust been constant.

RESULTS AND DISCUSSION

Digital Computer Calculation

A digital computer program was developed which included the low thrust trajectory equations of the appendix, both thrust vector control methods, orbit shadowing, solar array power degradation, and the ion thruster throttling technique. Each trajectory calculation results in time histories of orbital elements, shadow time in each orbit, thruster parameters, thrust vector control angle, and solar array parameters. The initial solar array size was adjusted for each initial payload and altitude until that solar array size was found which resulted in 5 kilowatts of power after 5 years of operation.

Solar Array Power Degradation

A typical power degradation curve during an ascent trajectory is shown in figure 6. A full power of 7.5 kilowatts is available to the three thrusters only for about 3 days, whereupon the throttling commences and the available 5 kilowatt power line is approached. As an alternative procedure, it may be advantageous to shut down one of the thrusters around the 50 day point, thereby maintaining high beam currents and the high thruster efficiencies which result. At this time, power is available to support only two thrusters at their full input power of 2.5 kilowatts each. In addition, since it has few operating hours, the thruster shut down could become a backup to the two thrusters which continue to operate. The rapidity with which the power level reaches 5 kilowatts is generally true for this payload range and launch vehicle. For launch vehicles which place the same payload

range into higher parking orbit altitudes, the slope of the power degradation curves is not as severe.

Control Angle Variation

Figure 7 presents an example of (for one payload and trajectory) the variation of the control angle β with the semimajor axis which is required to accomplish the concurrent change of inclination and semimajor axis indicated. At the beginning of the ascent the thrust vector is required to sweep through 53° the instant the spacecraft passes through the antinodes. At the end of the ascent, the sweep is over 140°. In actuality, this sweep could not be performed instantaneously. The true optimal solution as described in reference 4 employs a thrust vector control resembling a sine wave of orbit revolution periodicity and reversing its out of plane direction at the antinodes. The sweep about the antinodes would then more likely resemble the true optimal solution or at worst be a ramp through the antinode. The performance results which follow should therefore be considered conservative.

Transfer Time Requirements

The performance results which follow are shown as a function of the synchronous payload mass m_s which is defined as

$$m_s = m_o - m_p \tag{7}$$

where m_o is the payload into the low altitude parking orbit and m_p is the low thrust propellant mass expended during the transfer. It may be of more interest to the mission planner to define the net spacecraft mass

$$m_n = m_o - m_{ps} - m_p - m_t = m_s - m_{ps} - m_t \tag{8}$$

using the nomenclature adopted in reference 10. The propellant tankage m_t is estimated to be 15 kilograms for this study. The propulsion system mass m_{ps} is composed of the power subsystem mass and the thruster subsystem mass. The mass of three thrusters is estimated at 30 kilograms. Because of the present intensive efforts to reduce the specific weight of solar arrays, the reader is left to estimate his own value of mass per kilowatt of solar array and m_s.

The transfer times required to place a given payload m_s into geosynchronous orbit for both thrust control methods is shown in figure 8. The additional transfer times

required because of orbit shadowing are shown on the dashed curve. For a given synchronous payload, the near optimal control method represents a 22 to 25 percent decrease in the transfer time associated with the sequential thrust vector control method.

Solar Array Size Requirements

Figure 9 shows the initial array sizes required to obtain a solar array power of 5 kilowatts after 5 years of operation for both the sequential and near optimal thrust vector controls. The near optimal control causes the spacecraft to remain in the intense regions of the radiation belt longer than the sequential control. Therefore, more array is necessary for the near optimal case than for the sequential case. The array sizes of figure 9 may be used in conjunction with figure 8 to determine the transfer times as a function of net payload.

A spacecraft directly injected into the geosynchronous orbit would require an initial solar array of approximately 7 kilowatts to ensure a 5 kilowatt power level at the end of the mission. Therefore, the amount of solar array in excess of 7 kilowatts in figure 9 would be chargeable to achieving geosynchronous orbit with electric propulsion.

As previously mentioned, no second stage propellant reserves were assumed in calculating the launch vehicle performance of figure 3. The propellant reserves were assumed to be appropriately split between the transfer orbit perigee and apogee burns to maintain a circular final parking orbit. If the actual launch vehicle performance is either worse than or better than expected, however, this procedure would result in the parking orbit having an eccentricity not greater than 0.02. Assuming the removal of the residual eccentricity was done at the synchronous altitude with 5 kilowatts of power to the thrusters, the time penalty would not be greater than 2 days and the payload penalty not greater than 2 kilograms.

The parking orbit altitudes are shown in figure 10 for the missions having the geosynchronous payloads given in figures 8 and 9.

CONCLUDING REMARKS

The performance of the TAT/Delta/Electric stage for geosynchronous orbit injection has been evaluated for two thrust steering programs when the power to the thrusters is degrading. Limited background has been given for the space radiation effect on solar power systems together with a technique for calculating the solar array power under this effect.

Two thrust vector control methods or steering programs have been evaluated. One program changes the orbital altitude and inclination sequentially while the other changes

these orbital elements concurrently. Compared on the basis of total geosynchronous payload, the second steering program offers a 22 to 25 percent decrease in the transfer time over that of the first steering program. The second steering program, however, requires a slightly larger (up to 2 percent) solar array. For a geosynchronous payload range of 450 to 1100 kilograms, the transfer times for the second steering program vary from 90 to 285 days. Over the same payload range, 8.5 to 10 kilowatts of solar array are required to produce a degraded solar array power of 5 kilowatts after 5 years of operation. This compares to an initial solar array of 7 kilowatts required for a direct injection mission.

Lewis Research Center,
National Aeronautics and Space Administration,
Cleveland, Ohio, August 24, 1971,
682-10.

APPENDIX - LOW THRUST TRAJECTORY EQUATIONS WITH ERROR ANALYSIS

The trajectory is simulated by finding the changes in the classical orbital elements per orbit revolution when the spacecraft is subjected to the low thrust perturbation. The changes in the orbit elements are derived from Lagrange's planetary equations which give the time rates of change of the osculating orbital elements as

$$\frac{da}{dt} = \frac{2\, e \sin\theta}{n\sqrt{1 - e^2}} R + \frac{2a\sqrt{1 - e^2}}{nr} S \tag{A1}$$

$$\frac{de}{dt} = \frac{\sqrt{1 - e^2}}{na} \sin\theta\, R + \frac{\sqrt{1 - e^2}}{na^2 e}\left[\frac{a^2(1 - e^2)}{r} - r\right] S \tag{A2}$$

$$\frac{d\Omega}{dt} = \frac{r \sin(\theta + \omega) W}{na^2\sqrt{1 - e^2}\sin i} \tag{A3}$$

$$\frac{di}{dt} = \frac{r \cos(\theta + \omega) W}{na^2\sqrt{1 - e^2}} \tag{A4}$$

$$\frac{dw}{dt} = \frac{r \sin(\theta + \omega)\cot i}{na^2\sqrt{1 - e^2}} W - \frac{\sqrt{1 - e^2}\cos\theta}{nae} R + \frac{\sqrt{1 - e^2}}{nae}\left(1 + \frac{1}{1 + e\cos\theta}\right)\sin\theta S \tag{A5}$$

where R is the low thrust acceleration directed along the radius vector, S the acceleration in the orbit plane and perpendicular to the radius vector with positive direction in the direction of the velocity vector, and W the acceleration normal to the orbit plane and in a direction to complete a right handed coordinate system.

For circular orbits, the radial component does not exist. We can now introduce the control angle β, the out-of-plane angle between the velocity vector and the thrust vector, into the equations by letting

$$S = F \cos\beta \tag{A6}$$

$$W = F \sin\beta \tag{A7}$$

where F is the total low thrust acceleration available from the ion thrusters. When equations (A6) and (A7) are substituted into equations (A1) to (A5), and integration is performed with respect to the true anomaly while assuming the elements are constant over a revolution, the change in the orbital elements per orbit revolution are given by

$$\Delta a = 4\pi a^3 \frac{F \cos \beta}{\mu} \quad \text{(rad)} \tag{A8}$$

$$\Delta e = 0 \tag{A9}$$

$$\Delta \Omega = 0 \tag{A10}$$

$$\Delta i = 4a^2 \frac{F \sin \beta}{\mu} \quad \text{(rad)} \tag{A11}$$

$$\Delta \omega = 0 \tag{A12}$$

where equations (A10) and (A11) are derived making the additional assumption that the normal acceleration is reversed at the antinodes. Corrections are made to equations (A8) to (A12) when the spacecraft is in Earth shadow.

The low thrust perturbation equations (A8) to (A12) are combined with the Earth oblateness perturbation equations

$$\Delta \omega = 3\pi J_2 \left(\frac{R}{a}\right)^2 \left(2 - \frac{5}{2} \sin^2 i\right) \quad \text{(rad)} \tag{A13}$$

$$\Delta \Omega = -3\pi J_2 \left(\frac{R}{a}\right)^2 \cos i \quad \text{(rad)} \tag{A14}$$

to model the low thrust spiral out. The total low thrust acceleration is calculated according to the method described in table II.

The results of the simplified program of equations (A8) to (A14) were compared with the results of a computer program which numerically integrates the equations of motion. The thrust to weight ratio selected represents the maximum for the thrust levels and payloads considered in this study. Both computer programs integrated the trajectory from a starting altitude of 12 000 kilometers until the geosynchronous altitude was reached. The results showed less than a 1 percent difference between the Δa as calculated by the closed form expressions of equations (A8) to (A14) and the Δa calculated by the numerical integration program over the same time interval.

REFERENCES

1. Ghosh, Ranjan; and Huson, George: Achievement of Synchronous Orbit Using Electric Propulsion. Paper 69-275, AIAA, Mar. 1969.
2. Reader, Paul D.; and Regetz, John D., Jr.: A Delta Boosted, Electrically Raised High Power Synchronous Satellite. Paper 69-1104, AIAA, Oct. 1969.
3. Hrach, Frank J.: Comparison of Solar-Electric Propulsion Systems for the Synchronous Equatorial Satellite-Raising Mission. NASA TM X-1936, 1970.
4. Edelbaum, Theodore N.: Propulsion Requirements for Controllable Satellites. ARS J., vol. 31, no. 8, Aug. 1961, pp. 1079-1089.
5. Cooley, William C.; and Barrett, Mathew J.: Handbook of Space Environmental Effects on Solar Cell Power Systems. Exotech, Inc., Jan. 1968.
6. Anon.: Solar Cell Space Manual. Centralab, Globe-Union, Inc.
7. Hrach, Frank J.: Optimum Specific Impulse for Electrostatic Engines Used for Satellite Raising to Synchronous Equatorial Orbit. NASA TM X-52568, 1969.
8. Bechtel, Robert T.: Performance and Control of a 30-CM-DIAM, Low-Impulse, Kaufman Thruster. J. Spacecraft Rockets, vol. 7, no. 1, Jan. 1970, pp. 21-25.
9. King, H. J.; and Poeschel, R. L.: Low Specific Impulse Ion Engine. Hughes Research Labs. (NASA CR-72677), Feb. 1970.
10. Anon.: Electric Propulsion Mission Analysis. NASA SP-210, 1969.

TABLE I. - INITIAL ION THRUSTER PARAMETERS

Input power, P_i, W	2500
Beam voltage, V_{net}, V	803
Beam current, I_B, A	2.43
Power losses, W	120
Discharge losses, eV/ion	170
Propellant utilization efficiency, η_u, percent	88
Electrical efficiency, η_e, percent	78
Specific impulse (system), I_{sp}, sec	2500
Thrust, T, mlb (mN)	31.6 (140.6)

TABLE II. - ION THRUSTER THROTTLING ASSUMPTIONS AND TECHNIQUE

Parameter	Remarks
Input power, P_i, W	Varies according to solar array power
Beam voltage, V_{net}, V	Constant
Beam current, I_B, A	Varies; $I_B = P_i \eta_e / V_{net}$
Power losses, W	Fixed at 120
Discharge losses, eV/ion	Fixed at 170
Propellant utilization efficiency, η_u	Varies linearly with beam current with a slope $d\eta_u / dI_B = 0.15$
Electrical efficiency, η_e	Varies; $\eta_e = \frac{1 - (\text{power losses/power})}{1 + (\text{discharge losses}/V_{net})}$
Specific impulse (system), I_{sp}, sec	Varies; $I_{sp} = 100\, \eta_u \sqrt{V_{net}}$
Thrust, T, mlb (mN)	$T = 45.9\, \eta_e \eta_u\, P_i / I_{sp}$ $(204.2\, \eta_e \eta_u\, P_i / I_{sp})$

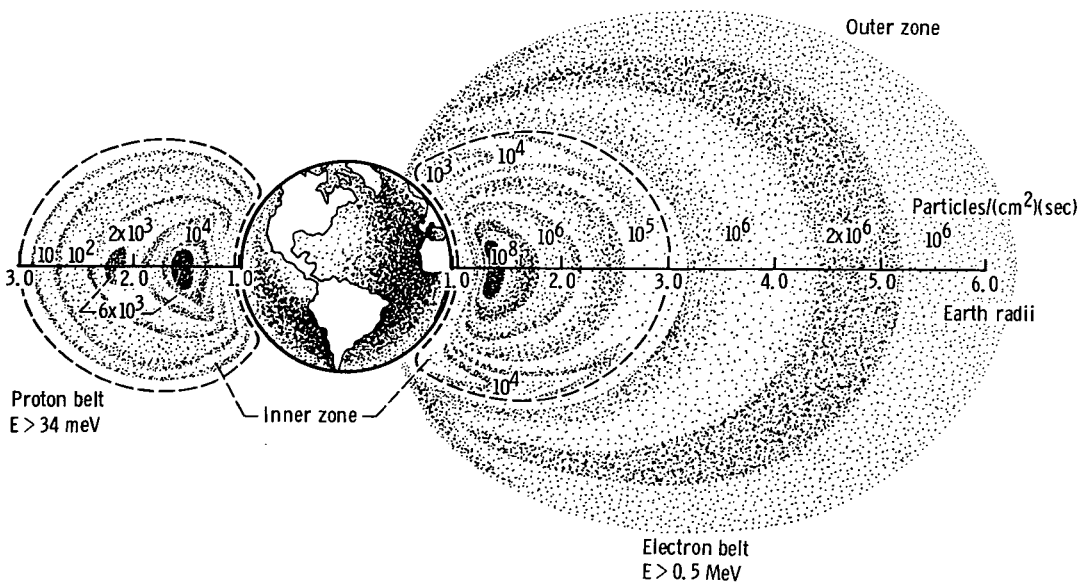

Figure 1. - Trapped radiation zones (Aerospace Medicine, Dec., 1969).

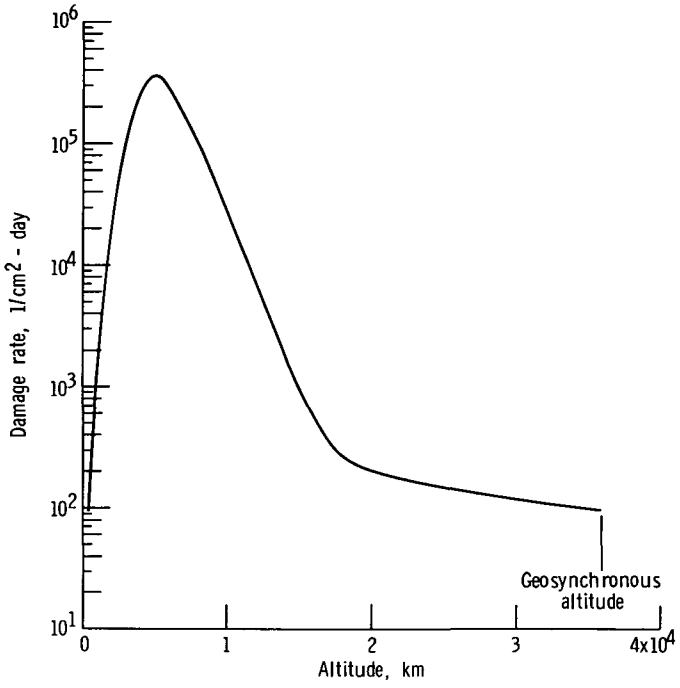

Figure 2. - Damage rates for 30^0 inclination, circular orbits.

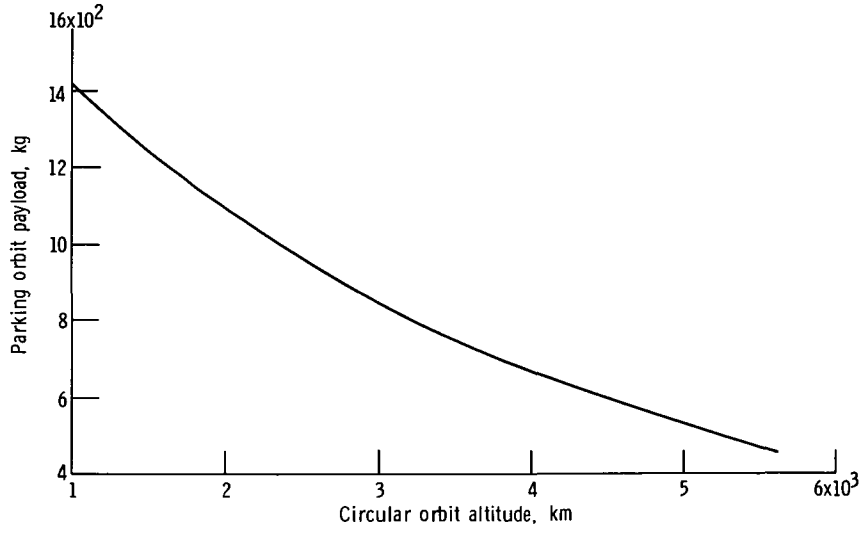

Figure 3. - Performance of TAT (9c)/Delta (transtage) vehicle for due east launch from Cape Kennedy.

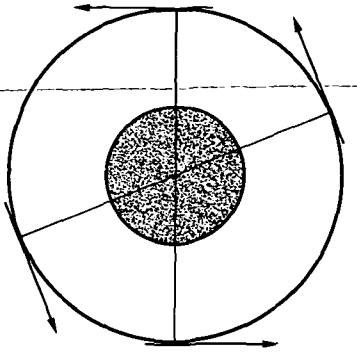

(a) Circumferential for altitude raising.

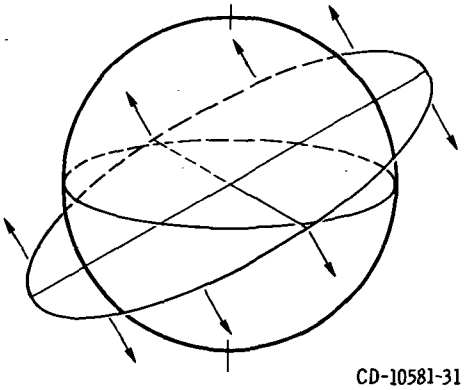

CD-10581-31

(b) Normal, switched at orbit antinodes for inclination change alone.

Figure 4. - Thrust programs for accomplishing various orbit changes.

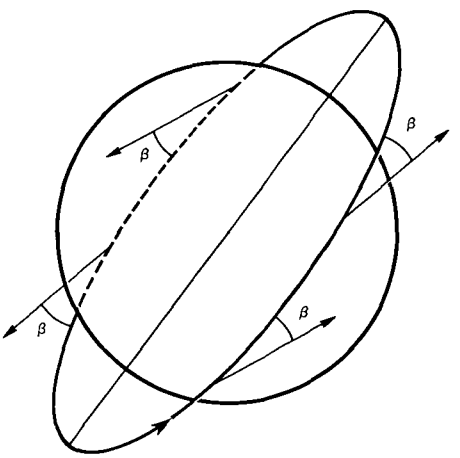

Figure 5. - Thrust program for accomplishing simultaneous altitude and inclination change.

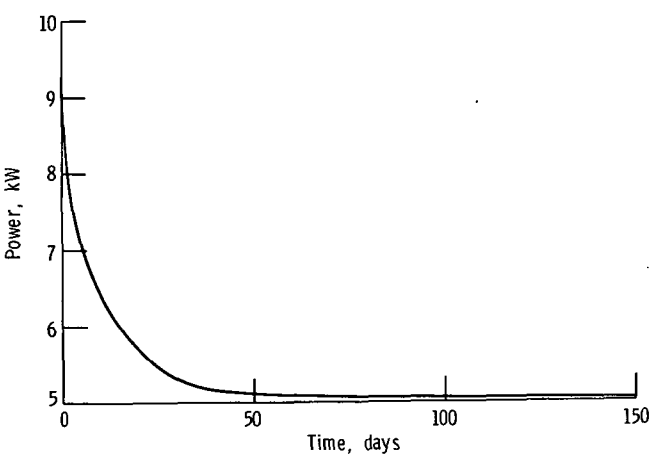

Figure 6. - Typical power degradations for spiral ascent.

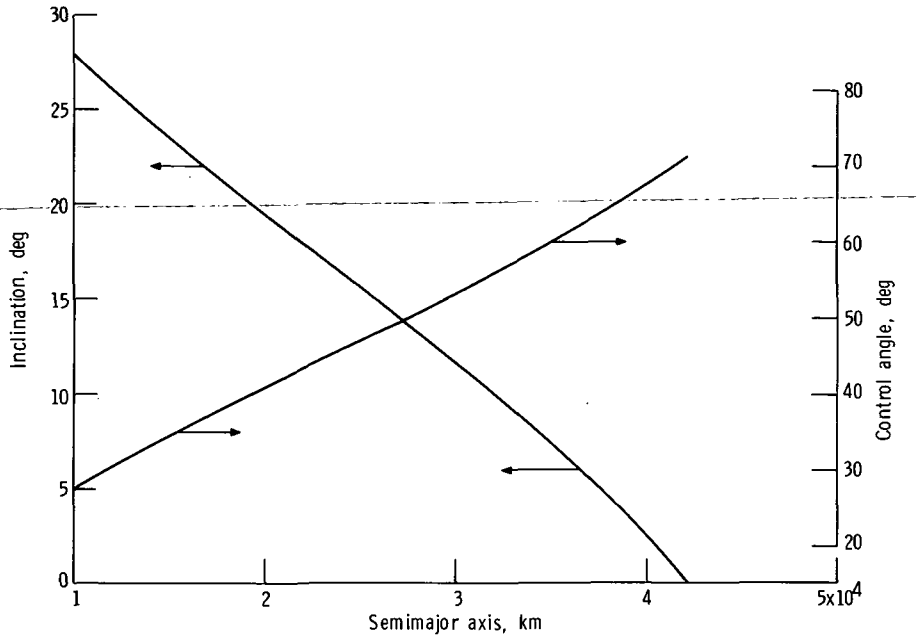

Figure 7. - Example of near optimal thrust control.

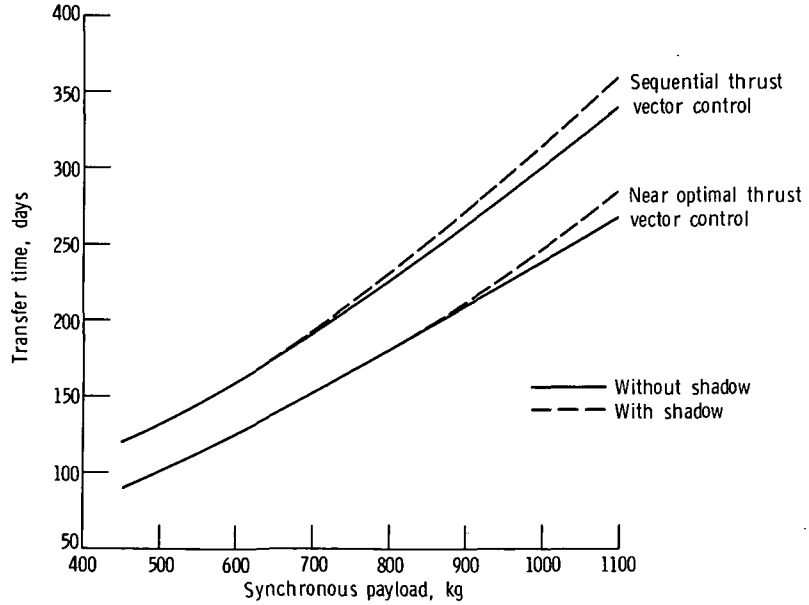

Figure 8. - Capability of solar electric propulsion stage to achieve 5-year mission life with 5 kilowatts of power remaining.

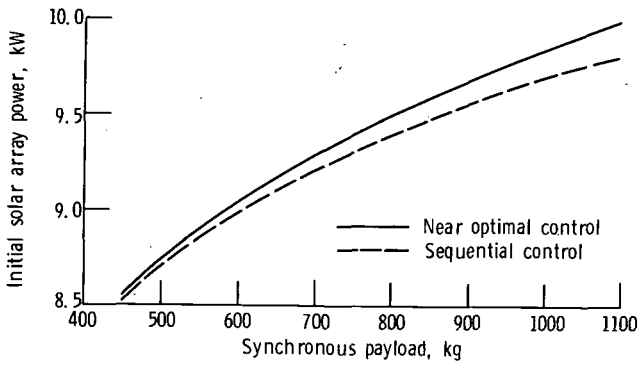

Figure 9. - Initial solar array size requirements.

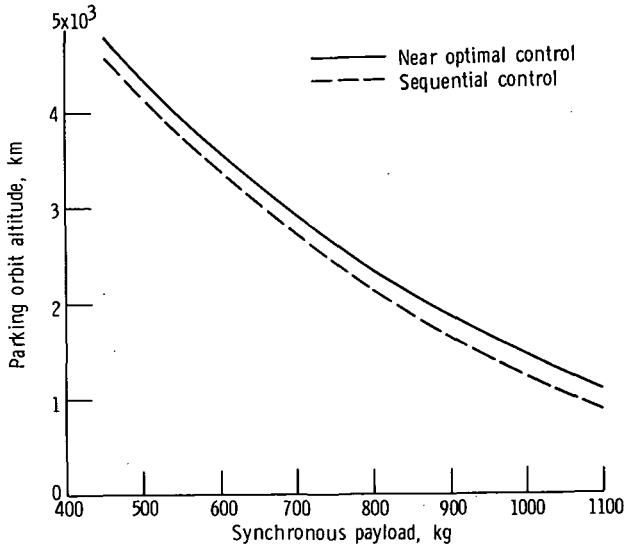

Figure 10. - Parking orbit altitudes for various synchronous payloads.

NASA-Langley, 1971 —— 30 E-6477

"The aeronautical and space activities of the United States shall be conducted so as to contribute . . . to the expansion of human knowledge of phenomena in the atmosphere and space. The Administration shall provide for the widest practicable and appropriate dissemination of information concerning its activities and the results thereof."

—NATIONAL AERONAUTICS AND SPACE ACT OF 1958

NASA SCIENTIFIC AND TECHNICAL PUBLICATIONS

TECHNICAL REPORTS: Scientific and technical information considered important, complete, and a lasting contribution to existing knowledge.

TECHNICAL NOTES: Information less broad in scope but nevertheless of importance as a contribution to existing knowledge.

TECHNICAL MEMORANDUMS: Information receiving limited distribution because of preliminary data, security classification, or other reasons.

CONTRACTOR REPORTS: Scientific and technical information generated under a NASA contract or grant and considered an important contribution to existing knowledge.

TECHNICAL TRANSLATIONS: Information published in a foreign language considered to merit NASA distribution in English.

SPECIAL PUBLICATIONS: Information derived from or of value to NASA activities. Publications include conference proceedings, monographs, data compilations, handbooks, sourcebooks, and special bibliographies.

TECHNOLOGY UTILIZATION PUBLICATIONS: Information on technology used by NASA that may be of particular interest in commercial and other non-aerospace applications. Publications include Tech Briefs, Technology Utilization Reports and Technology Surveys.

Details on the availability of these publications may be obtained from:

SCIENTIFIC AND TECHNICAL INFORMATION OFFICE

NATIONAL AERONAUTICS AND SPACE ADMINISTRATION

Washington, D.C. 20546